A twelve-year-long low-frequency earthquake catalog for Northern California

Ariane Ducellier[1], **Kenneth Creager**[1]

[1]University of Washington

Key Points:

- enter point 1 here
- enter point 2 here
- enter point 3 here

Corresponding author: Ariane Ducellier, ducela@uw.edu

Abstract

enter abstract here

1 Introduction

Tectonic tremor is a weak but persistent shaking of the Earth that has been discovered in many subduction zones and some strike-slip faults throughout the world. Tremor is observed on seismograms as apparent noise whose amplitude is modulated in time in a similar manner at stations that are dozens of kilometers apart from each other. It is characterized by a long (several seconds to many minutes), low amplitude seismic signal, emergent onsets, and an absence of clear impulsive phases. Tremor can be explained as a swarm of low-frequency earthquakes (LFEs), that is small magnitude earthquakes ($M \sim 1$) which dominant frequency is clearly low (1-10 Hz) compared with that of ordinary tiny earthquakes (up to 20 Hz). The source of the tremor and the LFEs is located on the plate boundary, and their focal mechanisms represent shear slip on a low-angle thrust fault dipping in the same direction as the plate interface (?, ?). LFEs are usually grouped into families of events, with all the earthquakes of a given family originating from the same small patch on the plate interface, and recurring more or less episodically in a bursty manner. In subduction zones such as Nankai and Cascadia, tectonic tremor and LFE observations are spatially and temporally correlated with slow slip observations (?, ?, ?). Due to this correlation, these paired phenomena have been called Episodic Tremor and Slip (ETS).

The relatively short recurrence of slow slip and tremor events results in a rich history both in space and time and reveals potential patterns. These event histories have allowed scientists to see complete event cycles, which is typically not possible to explore in traditional earthquake catalogs. However, most of the work on low-frequency earthquakes (LFEs) has been focused on detecting LFEs during periods of high tremor activity, grouping them into families of events, and locating the source of the LFE families. Longer catalogs (several years) have been established for LFE families in Mexico (two-year long catalog by ? (?)), the San Andreas Fault (fifteen-year-long catalog by ? (?)), Washington State (five-year-long catalog by ? (?) and two-year-long catalog by ? (?, ?)), New Zealand (eight-year-long catalog by ? (?)), and Japan (twelve-year-long catalog by ? (?) and eight-year-long catalog by ? (?)). These studies have shown that the recurrence behavior of LFE families varies a lot between seismic regions, and inside the same seismic region. In northern Washington, ? (?) have identified and characterized four different LFE families that span the width of the transition zone in the Cascadia Subduction Zone beneath western Washington State. They found that the LFEs swarm duration, recurrence interval, and event size decrease systematically with increasing depth. On the San Andreas Fault, ? (?)) observed a large diversity of recurrence behaviors among the LFE families, from semicontinuous to highly episodic. Particularly, two families exhibited bimodal recurrence patterns (about 3 and 6 days for the first one, and about 2 and 4 days for the second one). Moreover, he observed an increase in the LFE event rate after the 2004 Parkfield earthquake.

? (?)) have detected LFEs in southern Cascadia during the April 2008 ETS event using seismic data from the EarthScope Flexible Array Mendocino Experiment (FAME). They used a combination of autodetection methods and visual identification to obtain the initial templates. Then, they recovered higher signal-to-noise LFE signals using iterative network cross-correlation. They found that the LFE families on the southern Cascadia Subduction Zone were located above the plate boundary, with a large distribution of depths (28-47 km). Three additional LFE families were found on two strike-slip faults, the Maacama and Bucknell Creek faults, which are part of the San Andreas Fault zone.

When the hard work of detecting LFEs and identifying LFE families has been carried out, and enough (a few hundred) LFEs have been identified for a given family, a template waveform can be obtained by stacking all the waveforms corresponding to all the LFEs identified. Once a template is available, additional LFEs can be found by cross-

correlating seismic data with the template, and assuming that an LFE is occurring whenever the value of the cross-correlation is higher than a chosen threshold. The signal-to-noise ratios are low, so LFEs can be best identified by stacking the cross-correlation functions of multiple stations. In this study, we first use the catalog established by ? (?) for the months of March and April 2008 to create templates for the temporary seismic stations of the FAME experiment. We then use these templates to extend the catalog to the whole period when the FAME experiment was running, between July 2007 and June 2009. Next, we use the LFEs detections from the 2007-2009 periods to create templates for the permanent stations of three seismic network in northern California. These new templates allow us to extend the LFE catalog to the period XXX-XXX.

Add something about the conclusions

2 Data

We used both seismic data from the temporary EarthScope Flexible Array Mendocino Experiment (FAME) distributed by Incorporated Research Institutions for Seismology (IRIS), and seismic data from three permanent seismic networks distributed by the Northern California Earthquake Data Center (NCEDC). The FAME network was installed in northern California between July 2007 and June 2009. The three permanent networks are Berkeley Digital Seismic Network (BK), Northern California Seismic Network (NC), and Plate Boundary Observatory Strain and Seismic Data (PB). We used both one-component and three-components seismic stations. Depending on availability, we used channels BHZ, EHZ, HHZ, or SHZ as we are mainly interested in the frequency band 1-10Hz. We restricted ourselves to seismic stations less than 100 kilometers away from the epicenter of an LFE family, as we do not expect to have good signal-to-noise ratio for stations located farther away. The complete list of seismic stations and channels used in this study is given in the Supplementary Material. Figure XXX shows a map of the locations of the LFE families, and of the locations of the seismic stations. We can see that we have a good coverage of the area, and most LFE families are surrounded by several seismic stations.

? (?) have kindly accepted to share their LFE catalog with us. They have provided a list of 66 LFE families with, for each family, the location of the hypocenter of the family, the list of stations and channels used to detect LFEs for this family, and the timing of LFE detections. ? (?) have later reduced the number of LFE families to 37, by grouping together families with many common detections, but we chose to use the initial detections to extend the catalog. Using this dataset, we have created LFE templates for each LFE family and each seismic station and channel. For a given LFE family, a given station and a given channel, we downloaded an 80-second-long seismic waveform starting 10 seconds before the LFE detection time, we detrended the data, tapered the first and last 5 seconds of the data with a Hann window, removed the instrument response, bandpassed filter between 1.5 and 9 Hz, resampled the data to 20 Hz, and cut the first and last 10 seconds of data to obtain a one-minute-long template. All these preprocessing operations are done with the Python package obspy. We then stacked linearly all the waveforms after normalizing each waveform with the root mean square (RMS) to obtain a waveform template for each station and each channel.

3 Method

We used a matched-filter algorithm to detect LFEs. For a given LFE family, we download one hour of seismic data. Then for each station and each channel, we cross-correlate the one-hour long signal with the one-minute-long template for the given station and channel. As the signal-to-noise ratio of the seismic data is low, we may not see obvious peaks in the cross-correlation signal. However, if we stack the cross-correlation signals for all the channels and all the stations, we can see peaks appearing. Whenever

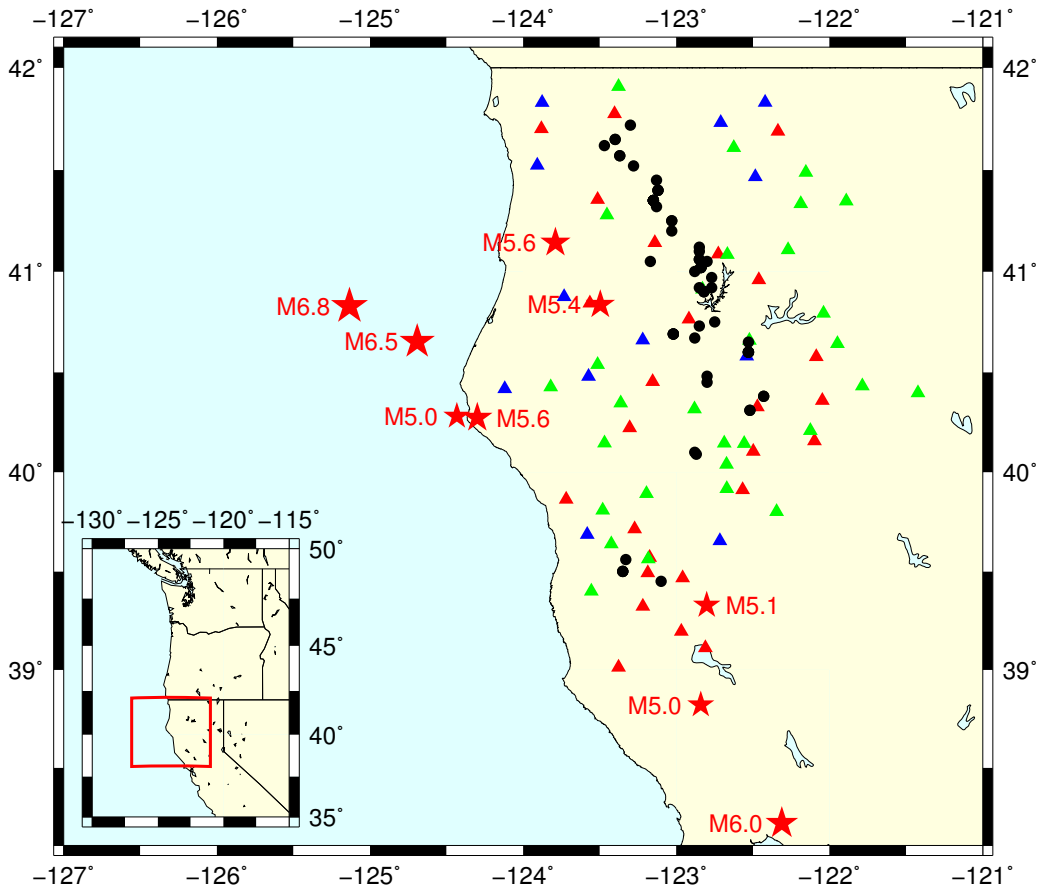

Figure 1. Map showing the location of the LFE families (back dots) and the seismic stations used in this study. Red triangles are the stations from the FAME experiment, green triangles are one-component permanent stations, blue triangles are three components permanent stations. Red stars are moderate ($M > 5$) nearby earthquakes.

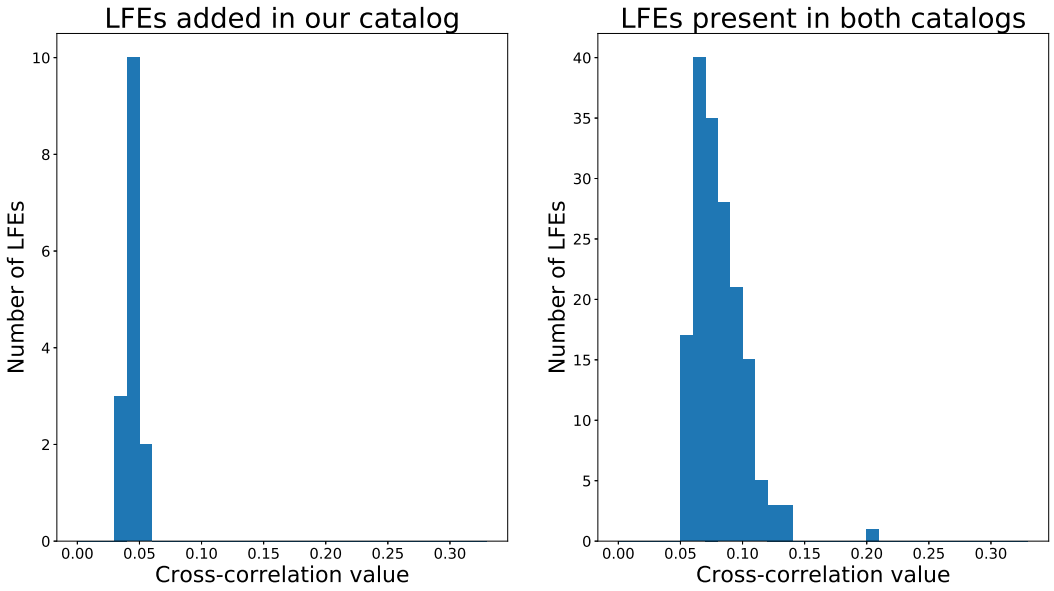

Figure 2. Cross-correlation values for LFEs added in the catalog for family 080413.07.023 (left) and cross-correlation values for LFEs in the original catalog from ? (?) (right). There were no missing LFEs for this family.

the value of the average cross-correlation is higher than a threshold (we chose a threshold equal to eight times the median absolute deviation of the stacked cross-correlation), we assumed that there is an LFE. As two peaks separated by a short period of time may actually correspond to the same LFE, we kept only LFEs that are separated by at least one second and, when two LFEs are separated by less than one second, we keep only the one with the higher value of the stacked cross-correlation.

We first looked for LFEs during the months of March and April 2008, which correspond to the period covered by the catalog from ? (?), and compared our detections with the initial detections from the original catalog of 66 families. For 19 families, we recovered all the LFE detections initially present in the ? (?)'s catalog. For 61 families, we recovered more than 90 % of the initial LFE detections. We also added 74 % more LFEs to the catalog, but most of added LFEs have a low cross-correlation value and may be false detections. Figure XXX shows the cross-correlation values for the LFEs in the original catalog, and for the LFEs that we added to the catalog for family 080413.07.023.

We then looked for LFEs during the period from July 2007 to June 2009, which correspond to the period when the FAME experiment was operating. Using a threshold equal to eight times the median absolute deviation of the stacked cross-correlation may produce false detections, therefore we filtered the LFE detection times before visualizing the two-year-long catalog. As the number of seismic stations recording may change with time as the stations were progressively installed during Summer and Fall 2007, and then progressively removed during May and June 2009, we kept only LFE detections for which the product of the cross-correlation value by the number of stations recording at that time is higher than a threshold (equal to 0.1 times the number of stations used to detect LFEs for the given LFE family). The threshold is thus different for each LFE family. The resulting LFE catalog for the period 2007-2009 is shown in Figure XXX. For comparison, we also plotted the tremor detection times from ? (?).

We note that there is a good spatial and temporal agreement between tremor and LFEs, with LFEs detected during the main tremor episodes. Additional small LFE episodes are also detected between bigger tremor episodes. The LFE families located south on

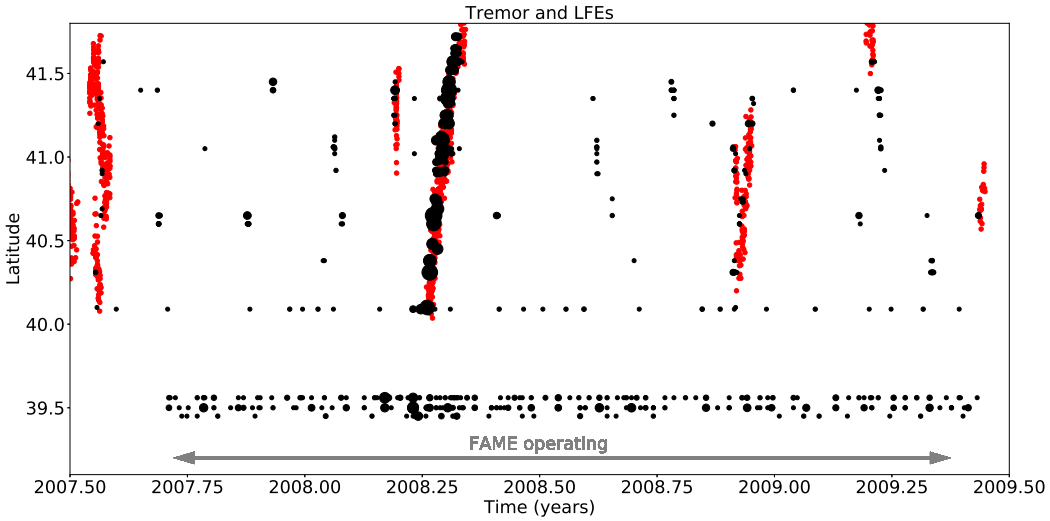

Figure 3. LFE and tremor detections as a function of time and latitude. Red dots represent tremor detections from the catalog of ? (?). Black dots represent days where LFEs are detected for a given LFE family. The size of the black dots are proportional to the number of LFEs detected during this day. The double-headed grey arrow represents the time period when the FAME experiment was operating at full capacity. LFE families south of 40 N latitude are on the San Andreas fault system.

the strike-slip fault from the San Andreas Fault system are much more active than the LFE families located on the subduction zone. Additionally, one LFE family located on the southern end of the subduction zone is also more active than families located farther north, and behaves more similarly to the strike-slip fault families.

We then used the LFE detections from the 2007-2009 catalog to make new templates for the permanent stations of the three seismic networks: Berkeley Digital Seismic Network (BK), Northern California Seismic Network (NC), and Plate Boundary Observatory Strain and Seismic Data (PB). For a given LFE family, we took the 150 LFE detection times with the best cross-correlation value, we downloaded one minute of seismic data around each detection, and linearly stacked the waveforms to obtain the templates. We looked for templates for both one-component stations and three-component stations.

For most families, we find that we can obtain good templates with signal-to-noise ratio for several stations. Only nine families have four or less seismic stations with good templates. Examples of templates are given in Figure XXX for station WDC and family 080401.05.050. To obtain the above catalog, we used one-minute-long templates, which included noise before and after the seismic wave arrivals. To increase the cross-correlation values between the templates and the data, we thus reduced the length of the templates to 25 to 40 seconds, depending on the maximum distance from the source to the stations. We did not use stations more than 100 kilometers away from the epicenter of an LFE family, as the template would be unlikely to have a good signal-to-noise ratio.

First comparison with 2007-2009 catalog with FAME data

4 Results

Now extension of the catalog, we will try 1995-2011.

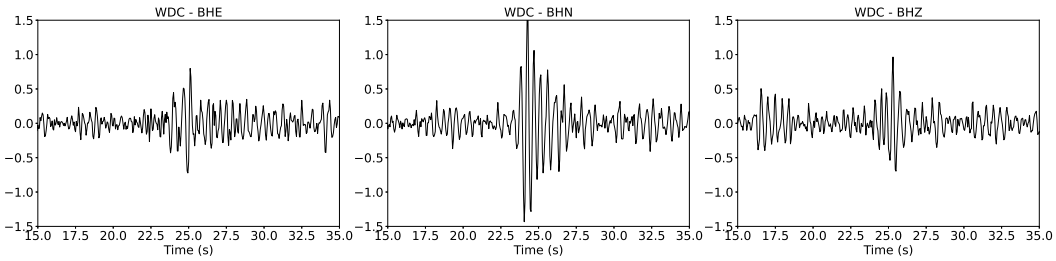

Figure 4. Low-frequency earthquake template for station WDC and family 080401.05.050 for the three channels BHE, BHN and BHZ (left to right). We can clearly see a P-wave arrival and an S-wave arrival about 7 seconds later. The P-wave has a higher amplitude on the vertical component, and the S-wave has a higher amplitude on the horizontal components.

New templates? New catalog? probably no time (or money)

5 Discussion

Section on effects of nearby earthquakes. Possible rapid tremor reversals

6 Conclusion

Acknowledgments

The authors would like to thank A. Plourde for sharing his low-frequency earthquake catalog. This project was funded by NSF grant XXX. A.D. would like to thank the Integral Environmental Big Data Research Fund from the College of the Environment of University of Washington, which funded cloud computing resources to carry out the data analyses. The seismic recordings used for this analysis can be downloaded from the IRIS and NCEDC websites.

References

Baratin, L., Chamberlain, C., Townend, J., & Savage, M. (2018). Focal mechanisms and inter-event times of low-frequency earthquakes reveal quasi-continuous deformation and triggered slow slip on the deep Alpine Fault. *Earth and Planetary Science Letters*, *484*, 111-123.

Boyarko, D., Brudzinski, M., Porritt, R., Allen, R., & Tréhu, A. (2015). Automated detection and location of tectonic tremor along the entire Cascadia margin from 2005 to 2011. *Earth and Planetary Science Letters*, *430*, 160-170.

Chestler, S., & Creager, K. (2017a). Evidence for a scale-limited low-frequecny earthquake source process. *Journal of Geophysical Research: Solid Earth*, *122*, 3099-3114. (doi:10.1002/2016jb013717)

Chestler, S., & Creager, K. (2017b). A model for low-frequency earthquake slip. *Geochemistry, Geophysics, Geosystems*, *18*, 4690-4708. (doi:10.1002/2017gc007253)

Frank, W., Shapiro, N., Husker, A., Kostoglodov, V., Romanenko, A., & Campillo, M. (2014). Using systematically characterized low-frequency earthquakes as a fault probe in Guerrero, Mexico. *Journal of Geophysical Research: Solid Earth*, *119*, 7686-7700.

Ide, S., Shelly, D., & Beroza, G. (2007). Mechanism of deep low frequency earthquakes: Further evidence that deep non-volcanic tremor is generated by shear

slip on the plate interface. *Geophysical Research Letters*, *34*, L03308.

Nakamura, M. (2017). Distribution of low-frequency earthquakes accompanying the very low frequency earthquakes along the Ryukyu Trench. *Earth, Planets, and Space*, *69*(1), 1-17.

Obara, K. (2002). Nonvolcanic deep tremor associated with subduction in southwest Japan. *Science*, *296*(5573), 1679-1681.

Ohta, K., & Ide, S. (2017). Resolving the detailed spatiotemporal slip evolution of deep tremor in Western Japan. *Journal of Geophysical Research: Solid Earth*, *122*(12), 10009-10036.

Plourde, A., Bostock, M., Audet, P., & Thomas, A. (2015). Low-frequency earthquakes at the southern Cascadia margin. *Geophysical Research Letters*, *42*, 4849-4855.

Rogers, G., & Dragert, H. (2003). Tremor and slip on the Cascadia subduction zone: The chatter of silent slip. *Science*, *300*(5627), 1942-1943.

Shelly, D. (2017). A 15 year catalog of more than 1 million low-frequency earthquakes: Tracking tremor and slip along the deep San Andreas Fault. *Journal of Geophysical Research: Solid Earth*, *122*, 3739-3753.

Sweet, J., Creager, K., Houston, H., & Chestler, S. (2019). Variations in Cascadia low-frequency earthquake behavior with downdip distance. *Geochemistry, Geophysics, Geosystems*, *20*, 1202-1217.